

24 **Abstract**

25 Vestigial organs are historical echoes of past phenotypes. Determining whether a
26 specific organ constitutes a functional or vestigial structure can be a challenging task,
27 given that distinct levels of atrophy may arise between and within lineages. The
28 mammalian pineal gland, an endocrine organ involved in melatonin biorhythmicity,
29 represents a classic example, often yielding contradicting anatomical observations.
30 In Xenarthra (sloths, anteaters and armadillos), a peculiar mammalian order, the
31 presence of a distinct pineal organ was clearly observed in some species (i.e.
32 Linnaeus's two-toed sloth) but undetected in other closely related species (i.e.
33 brown-throated sloth). In the nine-banded armadillo, contradicting evidence
34 supports either functional or vestigial scenarios. Thus, to untangle the physiological
35 status of the pineal gland in Xenarthra, we used a genomic approach to investigate
36 the evolution of the gene hub responsible for melatonin synthesis and signaling. We
37 show that both synthesis and signaling compartments are eroded and were lost
38 independently. Additionally, by expanding our analysis to 157 mammal genomes we
39 offer a comprehensive view showing that species with very distinctive habitats and
40 lifestyles have convergently evolved a similar phenotype: Cetacea, Pholidota,
41 Dermoptera, Sirenia and Xenarthra. Our findings suggest that the recurrent
42 inactivation of melatonin genes correlates with pineal atrophy, and endorse the use
43 of genomic analyses to ascertain the physiological status of suspected vestigial
44 structures.

45

46 **Keywords:** Gene Loss; Vestigiality; Pineal Gland; Xenarthra

47

48

49

50

51

52

53

54

55

56

57

58

59

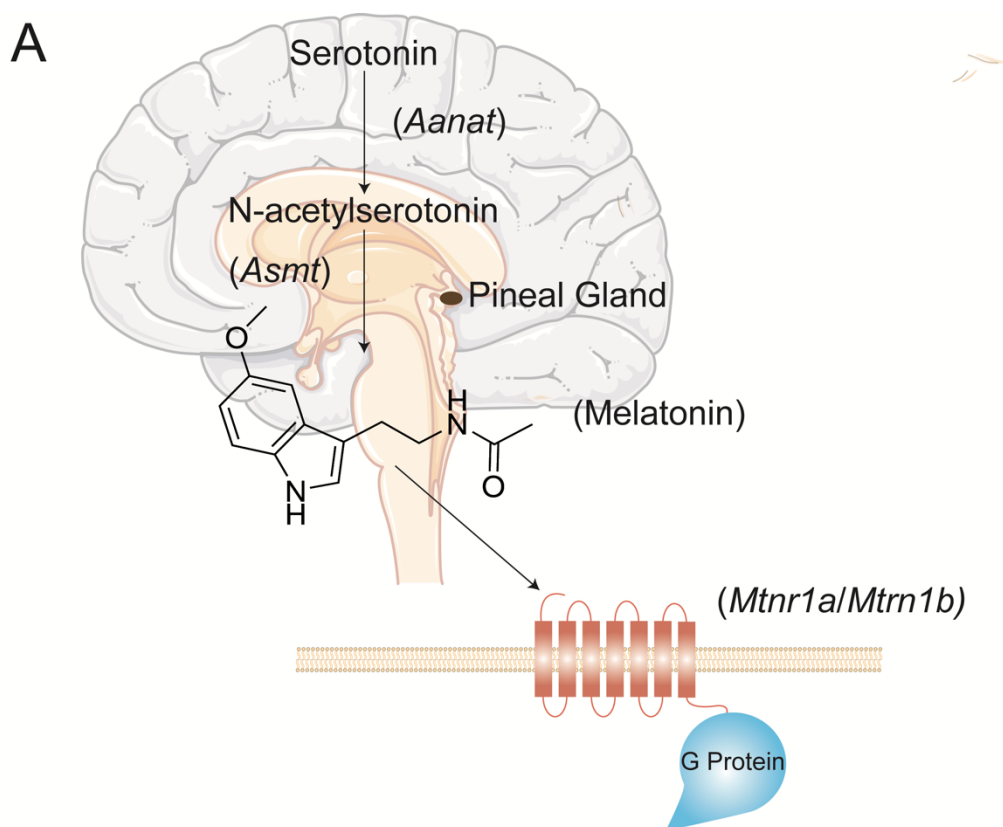
60 1. Introduction

61 Understanding the evolution of organ reduction, atrophy or indeed complete loss is
62 a fascinating quest, dating back to the seminal work of Charles Darwin, *On the Origin*
63 *of Species* (Darwin, 1859). Yet, to identify a structure as vestigial, described as a trait
64 with no function, operating sub-optimally, or even with a modified function from that
65 originally served, is no easy undertaking (Werth, 2014; Allmon & Ross, 2018): often
66 yielding contradictory anatomical descriptions (e.g., Jacob et al., 2000; Nweeia et al.,
67 2012). The increasing availability of whole genome sequences, on the other hand,
68 provides novel tools to untangle genomic signatures impacting organ reduction or
69 loss (e.g. Zoonomia Consortium, 2020). A key question is thus to understand how
70 genomic changes impact these processes. Among such signatures we find, more
71 commonly than initially anticipated, gene loss episodes: such as in the morphological
72 simplification of the urochordate *Oikopleura dioica*, the eye regression observed in
73 cave-dwelling populations of the teleost *Astyanax mexicanus*, the loss of gastric
74 glands in disparate vertebrate species or the loss of sebaceous glands in some
75 mammalian lineages (e.g., Olson, 1999; Castro et al., 2014; Albalat & Cañestro, 2016;
76 Cronk, 2009, Guijarro-Clarke et al. 2020; McGaugh et al., 2014; Springer et al. 2018;
77 Lopes-Marques et. a 2019a; Themudo et al., 2020; Springer et al., 2021).

78 A remarkable example of inconsistent observations in the functionality *versus*
79 vestigiality of an organ can be found in the anatomical observations of the pineal
80 gland in mammals (Ralph, 1975). The pineal gland is a small endocrine organ present
81 in the brain and playing a central role in the development of entrainment behaviors
82 through the action of melatonin (circadian rhythmicity). From a physiological
83 standpoint, melatonin synthesis occurs in a specialized cell type, the pinealocyte,
84 through an enzymatic cascade involving the arylalkylamine *N*-acetyltransferase
85 (*Aanat*) and *N*-acetylserotonin methyltransferase (*Asmt*) enzymes (Klein et al., 1997;
86 Simonneaux & Ribelayga, 2003); subsequent signaling uses a set of high affinity
87 receptors, *Mtnr1A* and *Mtnr1B*, involved in the response of the clock machinery to
88 melatonin stimulation, leading to local and overt phase shifts (Figure 1) (Axelrod et
89 al., 1964; Lewy et al., 1980; Reppart et al., 1996). Although anatomical studies clearly
90 support a well-defined pineal gland in most mammals, in lineages such as cetaceans,
91 mole rats and sirenians a true pineal gland seems to be absent; yet, some equivocal

92 observations exist, ranging from complete absence to detectable presence of this
93 gland in some species or in individuals within a species (Ralph, 1975; Ralph et al., 1985;
94 Kim et al., 2011; Panin et al., 2012). Conflicting evidence reporting measurable levels
95 of circulating melatonin (i.e. bottlenose dolphin) shed further doubt (Panin, 2012).
96 Interestingly, gene loss signatures were identified in these lineages, supporting the
97 loss-of-function of melatonin synthesis, a hallmark of pineal function, and/or
98 signalling (Fang et al., 2014; Huelsmann et al., 2019; Lopes-Marques et al., 2019b),
99 further demonstrating the power of genome analysis towards the clarification of
100 organ function. The presence of a functional pineal gland is also contentious in
101 Xenarthrans (armadillos, anteaters and sloths), a relatively understudied taxonomic
102 group characterized by its intriguing nature (Figure 1; Oksche, 1965; Benítez et al.,
103 1994; Superina & Loughry, 2015; Freitas et al., 2019) and representing one of the
104 earliest-branching clades of placental mammals (Murphy et al., 2007; O’Leary et al.,
105 2013). Xenarthrans are considered *imperfect* homeotherms, given their poor ability
106 to adjust body temperature (Mc Nab, 1979; 1980; 1985). This inaptitude for thermal
107 regulation, possibly related with their low metabolic rate and low energetic content
108 diet, makes Xenarthrans’ activity patterns highly affected by air temperature, with
109 potential effects in their circadian cycles (Chiarello, 1998; Giné et al., 2015; Maccarini
110 et al., 2015; Di Blanco et al., 2017). While a recent report clearly identified pineal glands
111 in the six-banded armadillo (*Euphractus sexcinctus*), Linnaeus’s two-toed sloth
112 (*Choloepus didactylus*), and in the southern tamandua (*Tamandua tetradactyla*), a
113 distinct pineal was not found or was reported missing in species such as southern
114 long-nosed armadillo (*Dasypus hybridus*), pale-throated sloth (*Bradypus tridactylus*),
115 giant anteater (*Myrmecophaga tridactyla*) or big hairy armadillo (*Chaetophractus*
116 *villosus*) (Benítez et al., 1994; Ferrari, 1998; Freitas 2019). However, in the nine-banded
117 armadillo (*Dasypus novemcinctus*) inconsistent reports advocate for either the
118 presence or absence of a genuine pineal gland (Harlow et al., 1981; Freitas et al., 2019).
119 Also, variable concentrations of circulating serum melatonin during the 24 h day–
120 night cycle have been detected in this species, raising the hypothesis of an
121 extrapineal source for melatonin production (Figure 1; Harlow et al., 1981; 1982). With
122 the emergence of various whole-genome sequences from Pilosa (sloths and
123 anteaters) (e.g., Uliano-Silva et al., 2019) and Cingulata (armadillos) (e.g., Lindblad-

124 Toh et al., 2011), Yin (et al., 2021) have recently reported the molecular erosion of
 125 *Aanat* in *Xenarthra*; yet, no attempt was made to expand this analysis to the full
 126 melatonin-related gene hub. Thus, we are now able to interrogate whether the gene
 127 repertoire of circadian rhythmicity is modified in this lineage and clarify the
 128 physiological status of the pineal gland within this group.
 129



B

Order	Melatonin Blood levels	Pineal Gland Anatomy	Habits
Cingulata	Circadian	Inconclusive	Cathemeral
Pilosa	No information	Inconclusive	Cathemeral

130
 131 Figure 1: Melatonin synthesis and signaling. Melatonin, generally described as a phase marker of the
 132 circadian clock, is initially synthesized from tryptophan which is converted in serotonin (Pévet, 2002).
 133 The final steps of this synthetic pathway include a two-step metabolization of the intermediate
 134 serotonin into melatonin, a process catalyzed by *Aanat* and *Asmt* (Klein et al., 1997; Simonneaux &
 135 Ribelayga, 2003). In mammals, *Mtnr1a* and *Mtnr1b* receptors, are involved in the response of the clock
 136 machinery to melatonin stimulation (Reppart et al., 1996) (A). Summary of the available information

137 regarding Xenarthran's melatonin levels, pineal gland presence and habits (B). (Illustrations used
138 elements from Servier Medical Art: <https://smart.servier.com/>)

139

140 **2. Material and Methods**

141 **2.1 Sequence collection**

142 To clarify the functional status of *Aanat*, *Asmt*, *Mtnr1a* and *Mtnr1b* in 8 Xenarthran
143 species (Supplementary Data 1), the genomic *loci* were retrieved for gene annotation
144 using three strategies (e.g. Alves et al., 2019; Lopes-Marques et al., 2019b): a) for
145 species with annotated genes, the genomic sequence of the target gene (ranging
146 from the upstream to the downstream flanking genes) was collected directly from
147 NCBI; b) for species with annotated genomes but lacking the annotation of the target
148 gene, the genomic region between two conserved flanking genes (downstream and
149 upstream) was directly collected and c) for unannotated genomes, blastn searches
150 were performed, using as query a set of three genes, including *Homo sapiens* (human)
151 target gene coding sequence (CDS), as well as those of the flanking genes in the same
152 species. From the blast results, the best matching genome scaffold corresponding to
153 the consensus hit across those obtained per each query sequence was retrieved.
154 When no consensual blast hit was obtained, all hits corresponding to the *H. sapiens*
155 CDS query were inspected, the aligning regions submitted to a back-blast search
156 against the nucleotide database of NCBI, with the matching genomic sequence
157 corresponding to the gene of interest being the one selected (when existing). When
158 several matchings were found, the best genomic scaffold (yielding the highest query
159 coverage and identity value) was collected for annotation.

160 For the 156 non-Xenarthran mammals with annotated genomes (Supplementary Data
161 1), the first two strategies described above were adopted to obtain the genomic
162 region corresponding to the target gene. In Dugong (*Dugong dugon*), since no
163 annotation is currently available, the genomic sequence containing the target gene
164 was retrieved *via* blastn searches.

165

166 **2.2 Gene Annotation and Mutational Validation**

167 The open reading frames of the mammalian orthologues of *Aanat*, *Asmt*, *Mtnr1a* and
168 *Mtnr1b* were investigated using *PseudoChecker* (pseudochecker.ciimar.up.pt), an

169 online platform suitable for gene inactivation inference (Alves et al., 2020). For this
170 purpose, the human gene orthologue was used as a comparative coding sequence
171 input (NCBI Accession ID regarding human *Aanat*: NM_001088.3; *Asmt*:
172 NM_001171039.1; *Mtnr1a*: NM_005958.4; *Mtnr1b*: NM_005959.5) to deduce the
173 coding status of a given candidate gene in each target species. By making use of
174 PseudoIndex - a user assistant metric built into the PseudoChecker pipeline that
175 rapidly estimates the erosion condition of the tested genes – putative ORFs of the
176 orthologous gene from each target species were assigned a discrete value from 0 to
177 5, with 0 suggesting a fully functional gene and 5 complete inactivation (Alves et al.,
178 2020). When PseudoIndex was higher than 2, we proceeded to manual annotation
179 and validation of possible disrupting mutations as previously described by Lopes-
180 Marques et al. (2019a, 2019b, 2019c). Briefly, by using *H. sapiens* CDS for each target
181 gene as reference, each exon was isolated and mapped to the genomic region of the
182 candidate pseudogenes using Geneious Prime (2019.2.3) “map to reference” tool.
183 The aligned regions were individually screened for ORF disrupting mutations (exon
184 deletions, sequence frameshifts and premature stop codons) and identified
185 mutations were annotated. Mutational validation was performed through retrieval
186 of raw sequencing reads in (at least) two independent Sequence Read Archive (SRA)
187 projects (when available).

188

189 **2.3 RNA-seq analysis**

190 Transcriptomic analysis was performed as previously described by Lopes-Marques (et
191 al., 2019c). Succinctly, RNA-seq datasets of multiple tissues were obtained from SRA
192 projects to inspect the functional condition of each target gene in Xenarthran species
193 (when available) and Human (*H. sapiens*) (Supplementary Data 2). Transcriptomic
194 reads recovered through blastn, were mapped to corresponding references
195 genomes using the “map to reference” tool from Geneious Prime (2019.2.3) and
196 manually removed if presenting poor alignment. Finally, reads were classified as
197 spliced reads (spanning over two exons), exon-intron reads or exonic reads
198 depending on the genomic region they mapped.

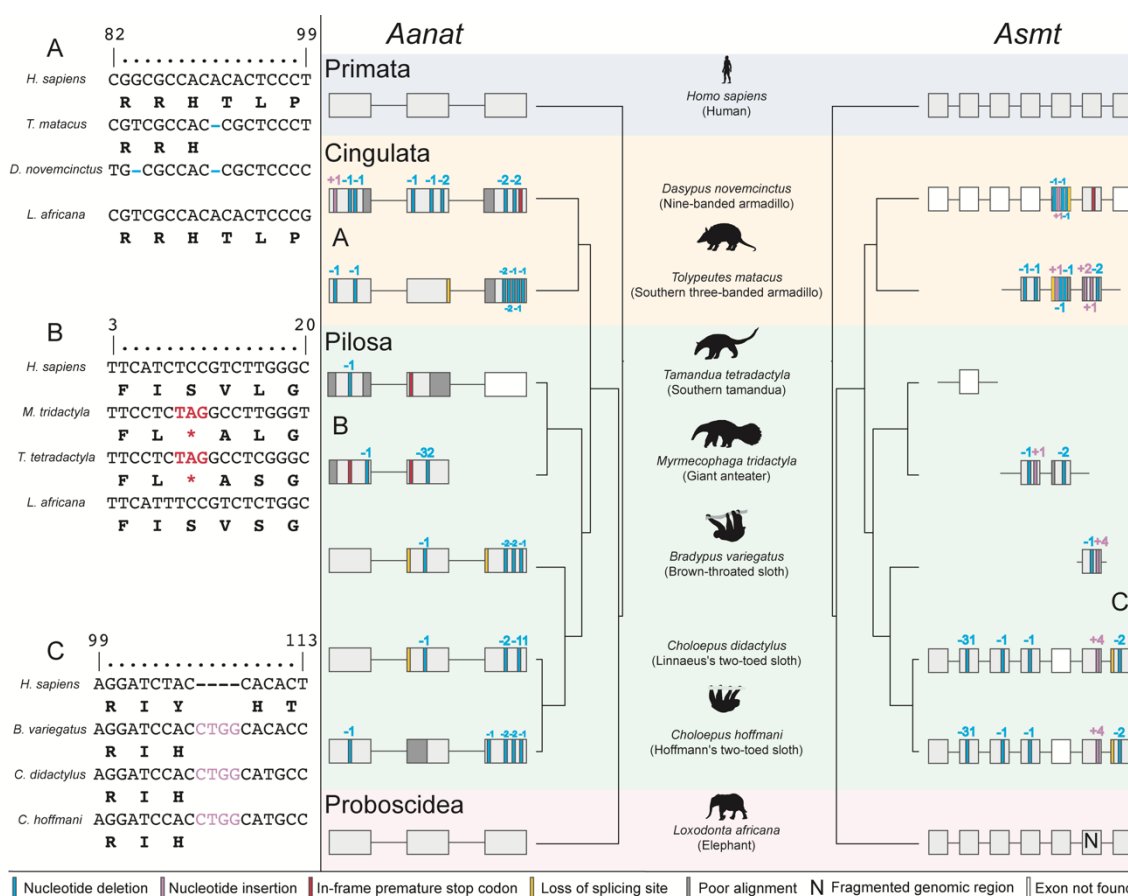
199

200 **3. Results**

201 **3.1 Erosion of melatonin-related genes in Xenarthra**

202 To infer the coding state of the melatonin synthesis genes in armadillos, anteaters
203 and sloths, we compared the genomic regions containing *Aanat* and *Asmt* in *H.*
204 *sapiens* to the full genomes of 8 eight Xenarthran species and *L. africana*
205 (Supplementary Data 1). Analysis using PseudoChecker (Alves et al., 2020), showed
206 that all analysed species presented a PseudoIndex equal to 5 (Supplementary Data 3)
207 - thus suggesting that the ORF of *Aanat* and *Asmt* includes inactivating mutations.
208 Subsequent manual annotation of all collected Xenarthran genomic sequences
209 revealed *Aanat* and *Asmt* gene erosion across all analysed species (Supplementary
210 Data 4). Regarding *Aanat*, in agreement with Yin (et al., 2021), we found numerous
211 ORF-disrupting mutations, including a conserved 1-nucleotide deletion in exon 1 in
212 Armadillos and a conserved 2-nucleotide deletion in exon 3 in Sloths (Figure 2;
213 Supplementary Data 4). On the other hand, although Yin (et al., 2021) were not able
214 to recover the genomic sequence containing the *Aanat* CDS in Anteaters, we
215 uncovered, among other disruptive mutations, a conserved in-frame premature stop
216 codon in exon 2. The identified mutations were next validated by searching at least
217 one ORF disruptive mutation per species in the corresponding SRAs; reads
218 corroborating the identified mutations were systematically found (Supplementary
219 Data 5). The analysis of *Asmt* in Xenarthra also revealed variable disruption patterns
220 across Xenarthra. In cingulatan, we found similar mutational events, however not
221 conserved within members of this group. Specifically, in *D. novemcinctus* exons 1 to 4
222 and 7 were not found, possibly due to poor genome coverage or complete exon
223 deletion (Figure 2). Moreover, in southern three-banded armadillo (*Tolypeutes*
224 *matacus*) several insertions/deletions (indels) have been identified in exon 6,
225 contrasting with *D. novemcinctus* where a validated in-frame premature stop codon
226 in the same exon was detected (Figure 2; Supplementary Data 4 and 6). In
227 *Vermilingua* (anteaters), we were only able to recover exons 4 and 5 in the Giant
228 anteater (*Myrmecophaga tridactyla*) which provide a range of mutations with
229 predicted disruptive effects (Figure 2; Supplementary Data 4). For Folivora (sloths),
230 across several identified ORF-disrupting mutations, a trans-species conserved 4-
231 nucleotide insertion in exon 6 was revealed and further validated by SRA searches
232 (Supplementary Data 4 and 6). RNA-Seq analysis in Linnaeus's two-toed sloth

233 (*Choloepus didactylus*) *Aanat* yielded a high proportion of exon-intron reads versus
 234 spliced reads, in clear contrast with the pattern found in *H. sapiens* (Supplementary
 235 Data 7). In the case of *Asmt*, no transcriptomic reads were recovered for *C. didactylus*.
 236 Similarly, SRA transcriptome searches were unable to retrieve reads of *D.*
 237 *novemcinctus* for both genes.
 238



239
 240 Figure 2: Schematic representation of the identified *Aanat* and *Asmt* genes ORF abolishing mutations
 241 in Xenarthra orders (Cingulata and Pilosa). Phylogenetic trees were calculated in www.timetree.org;
 242 last accessed March 13, 2021 using species list. Silhouettes were sourced from Phylopic
 243 (<http://phylopic.org>). Sequence alignments of the identified conserved disruptive mutations in both
 244 *Aanat* and *Asmt* genes of Xenarthra.

245
 246 We next examined the genes *Mtnr1a* and *Mtnr1b*, that encode G-protein coupled
 247 receptors responsible for melatonin signalling. In *D. novemcinctus*, the *Mtnr1a* coding
 248 status could not be accessed likely due to fragmentation of the respective genomic
 249 region (presence of sequencing gaps (Ns)). On the other hand, for both species
 250 comprising the two-toed sloth group (*Choloepus* sp.), we were able to identify a

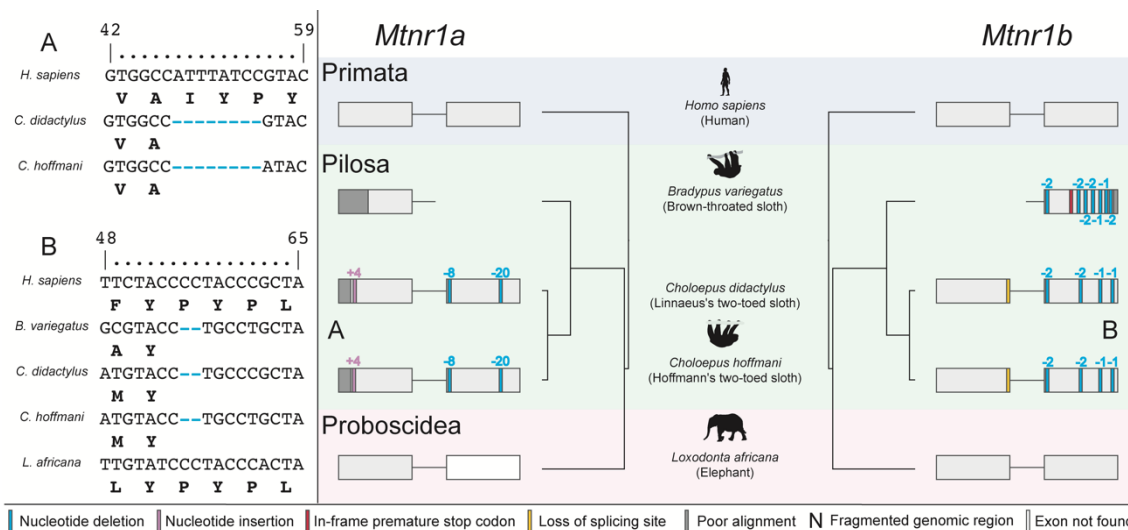
251 validated 8-nucleotide deletion and a 20-nucleotide deletion in exon 2 together with
252 a 4-nucleotide insertion in exon 1 (Figure 3; Supplementary Data 4 and 8). Curiously,
253 in elephant (*Loxodonta africana*) exon 2 was not found despite the completeness of
254 the assembly in the *Mtnr1a* region. The analysis of *Mtnr1b* CDS in *T. matacus* and
255 Screaming hairy armadillo (*Chaetophractus vellerosus*) uncovered several inactivating
256 mutations, including a conserved premature stop codon that truncates exon 2
257 (Figure 3). Pilosa species (sloths and anteaters) *Mtnr1b* gene annotation revealed the
258 presence of several ORF disrupting mutations, of note a single transversal mutation
259 present in all analysed species, namely a 2-nucleotide deletion in exon 2 (Figure 3;
260 Supplementary Data 4). This mutation was investigated and validated in both
261 *Choloepus* species (Supplementary Data 9). Searches for transcriptomic evidence for
262 *Mtnr1a* and *Mtnr1b* in *C. didactylus* retrieved a low number of reads, mostly
263 corresponding to immaturely mRNA (Supplementary Data 7).

264

265 **3.2 Melatonin-related genes are inactivated in other non-xenarthran mammals**

266 We next expanded our analysis to non-Xenarthran mammal genomes (157), to
267 address the coding status of *Aanat*, *Asmt*, *Mtnr1a* and *Mtnr1b* (Supplementary Data
268 1). Sequence search and analysis for *Aanat* returned a total of 11 species with no
269 annotation of a *Aanat*-like sequence: *Bison bison bison* (American bison), *Bos indicus*
270 (Zebu), *Bos mutus* (Wild yak), *Bubalus bubalis* (Water buffalo), *Camelus ferus* (Wild
271 bactrian camel), *Odocoileus virginianus texanus* (White-tailed deer), *Pantholops*
272 *hodgsonii* (Tibetan antelope), *Sus scrofa* (Wild boar), *Myotis davidii* (David's myotis)
273 and *Myotis lucifugus* (little brown bat). For the latter, we were not able to retrieve the
274 genomic locus containing the target gene, given that both upstream and
275 downstream flanking genes are also not annotated. Analysis using PseudoChecker
276 (Alves et al., 2020), showed that 32 species non-Xenarthran mammals presented a
277 PseudoIndex higher than 2 (Supplementary Data 3). From these species, members of
278 Cetacea (cetaceans) and Pholidota (pangolins) presented among their members, a
279 conserved (and validated) in-frame premature stop codon in Exon 1 (Supplementary
280 Data 4 and 10). Moreover, we also found ORF-disrupting mutations in Exon 1 of
281 velvety free-tailed bat (*Molossus molossus*), Kuhl's pipistrelle (*Pipistrellus kuhlii*) and
282 Sunda flying lemur (*Galeopterus variegatus*) with the latter being validated through

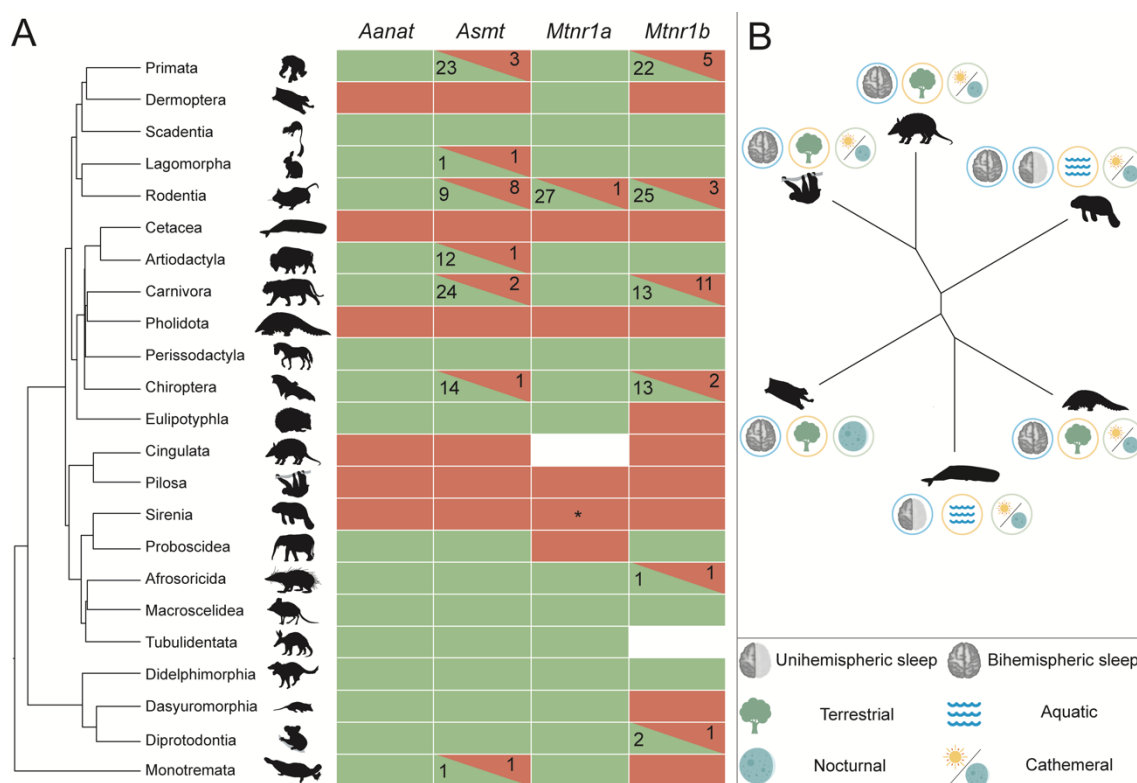
283 SRA genomic reads (Supplementary Data 4 and 10). In *D. dugon*, several disruptive
 284 mutations were identified, such as an eight-nucleotide insertion in exon 2 and the
 285 presence of a stop codon in exon 3 (Supplementary Data 4 and 10).
 286



287
 288 Figure 3: Schematic representation of the identified *Mtnr1a* and *Mtnr1b* genes ORF abolishing
 289 mutations in Xenarthra orders (Cingulata and Pilosa). Phylogenetic trees were calculated in
 290 www.timetree.org; last accessed March 13, 2021 using species list. Silhouettes were sourced from
 291 Phylopic (<http://phylopic.org>). Sequence alignments of the identified conserved disruptive mutations
 292 in both *Mtnr1a* and *Mtnr1b* genes of Xenarthra.

293
 294 Regarding *Asmt*, in 17 species the genomic fragments containing *Asmt*-like nucleotide
 295 sequences were not recovered given the lack of annotation for both target and
 296 flanking genes (Supplementary Data 3). For this gene, 74 species displayed a
 297 PseudoIndex higher than 2 (Supplementary Data 3), the majority due to
 298 fragmentation of the genomic region (presence of Ns), true absence of exons, poor
 299 alignment identity or incompleteness of the scaffold in the *Asmt* genomic region
 300 (Supplementary Data 4). Gene lesion events were found and validated mostly in
 301 Cetaceans, *G. variegatus*, *Manis* sp. (pangolins) and some Rodentia, with the latter
 302 showing poor alignment identity with the reference (Figure 4; Supplementary Data 4
 303 and 11). Other examples of species presenting disruptive mutations but with no SRA
 304 validation (given that no genomic independent SRAs projects are available) include
 305 Brandt's bat (*Myotis brandtii*), the Prairie vole (*Microtus ochrogaster*) with 2-
 306 nucleotide deletion in exon 1 and the Nancy Ma's night monkey (*Aotus nancymae*)

307 with single nucleotide deletions in exon 2 (Supplementary Data 4). In the case of *D.*
308 *dugon*, no ORF-disrupting mutations were found for *Asmt*, however, not all the exons
309 were recovered due to incompleteness of the scaffold (Supplementary Data 4).
310 We next expanded our search to understand whether melatonin signaling genes
311 would be compromised in non-Xenarthran mammals. For *Mtnr1a*, a total of 44 species
312 exhibited a PseudoIndex higher than 2 (Supplementary Data 3), yet manual curation
313 revealed ORF-disrupting mutations only in pangolins (validated through SRA
314 Projects; Supplementary Data 12) (Huelsmann et al., 2019), Hawaiian monk seal
315 (*Neomonachus schauinslandi*) and *D. dugon* (Supplementary Data 4). In cetaceans a
316 different scenario emerged, with several exons completely absent (Supplementary
317 Data 4) (Huelsmann et al., 2019; Lopes-Marques et al., 2019b).
318 In *Mtnr1b*, a total of 69 non-Xenarthran mammals displayed a PseudoIndex higher
319 than 2 (Supplementary Data 3). However, and contrary to the pattern found for
320 *Mtnr1a*, annotation of the collected sequences revealed *Mtnr1b* gene erosion across
321 multiple species, mostly affecting the Carnivora and Cetaceans but also Pholidota,
322 Sirenia and some Primates (Figure 4; Supplementary Data 4). Examples of conserved
323 inactivating mutations were found in bears (*Ursus sp.*) with an in-frame premature
324 stop codon in exon 1, weasels (*Mustela sp.*) sharing several indels in exon 2 and
325 pangolins with a single nucleotide deletion and an in-frame premature stop codon in
326 exon 1 (Supplementary Data 4 and 13). Other species with ORF-disruptive mutations
327 include *Nannospalax galili* (northern Israeli blind subterranean mole rat), exhibiting a
328 single nucleotide deletion in exon 1, *D. dugon* with a conserved fourteen-nucleotide
329 deletion in exon 2 or *G. variegatus* with an indel also in exon 1 (Supplementary Data 4
330 and 13). Detailed characterization of each target gene in mammals is available in
331 Supplementary Data 4 and the minutiae of SRA validation can be found in
332 Supplementary Data 10, 11, 12 and 13.
333



334

335 Figure 4: Mutational landscape of melatonin synthesis and signalling genes along the mammalian tree.

336 For each gene, we represented in green the orders where no ORF-disrupting mutations (frameshift

337 mutations, in-frame premature stop codons, loss of canonical splicing site or exon deletions) were

338 found across all members. On the other hand, orders where all members presented ORF-disrupting

339 mutations are highlighted in red. In orders (and in genes) with no consensual disruption pattern,

340 number of species presenting a coding/non-coding sequence were depicted respectively. Species

341 where no SRA validation was possible, were not included in this figure. * indicates the presence of

342 contradictory reports in *Mtnr1a* for *Trichechus manatus latirostris*. Phylogenetic relationships were

343 adapted from Vazquez et al. (2018). (A) Summary characterization of mammalian lineages presenting

344 complete molecular erosion of melatonin synthesis and signalling genes, regarding their sleep type,

345 habitat and lifestyle. (B)

346

347 4. Discussion

348 Here, we set out to investigate how evolutionary genomic signatures might untangle

349 the physiological status of controversial vestigial structures, using the pineal gland as

350 a case study (Pévet, 2002). For this, we addressed the evolution of a melatonin-

351 related gene hub, encompassing melatonin synthesis and signaling genes, in

352 Xenarthra and other mammals. Our results strongly suggest a complete landscape of

353 gene loss in Xenarthra, which further reinforce reports suggesting the lack of a pineal

354 gland in several members of this superorder (Quay, 1965; Harlow et al., 1981; Benítez

355 et al., 1994, Ferrari 1998; Freitas 2019). On the other hand, in species in which a pineal
356 gland was described (e.g., Freitas et al., 2019), the present data suggests that, despite
357 the anatomical observations, the canonical pineal gland physiology leading to
358 melatonin secretion is likely disrupted. Nevertheless, similarly to what was described
359 for *Tursiops truncatus* (bottlenose dolphin) (Panin et al., 2012), previous
360 radioimmunoassay methods have reported the presence of melatonin circulating in
361 *D. novemcinctus* (Harlow et al., 1981), implying either the existence of independent
362 pathways for melatonin synthesis and signaling (Slominski et al., 2003; Tan et al.,
363 2016) or possible acquisition of melatonin from food sources (Tan et al., 2010).
364 This strong genomic signature leading to the anatomical and/or physiological atrophy
365 of this endocrine gland might be viewed as an adaptive solution to overcome
366 physiological limitations. Described as cathemeral (irregular daily activity pattern)
367 and heterothermic species (Eisenberg & Redford, 1999) with limited capacity to
368 regulate their body temperature, Xenarthrans' movements are heavily influenced by
369 air temperature (Greggor, 1985; Camilo-Alves & Mourão, 2006; Giné et al., 2015; Attias
370 et al., 2018). Thus, to reduce such energetic costs, Xenarthrans may have suffered
371 reductive episodes, allowing behavioral strategies to overcome unfavorable
372 environmental conditions and mitigate thermal limitations (Yin et al., 2021).
373 Accordingly, convergent disruptive patterns with lineages also presenting labile body
374 temperature and suggestive bizarre sleeping patterns (Pholidota; Mc Nab, 1984;
375 Heath & Hammel, 1986; Weber et al., 1986; Imam et al., 2018; Yin et al., 2021) or living
376 in environments with specific thermal constraints (Cetacea and *Trichechus manatus*
377 *latirostris* (Florida manatee); Huelsmann et al., 2019; Lopes-Marques et al., 2019b; Yin
378 et al., 2021), make it plausible to hypothesize that, in these species, inactivation of
379 melatonin-related genes can be related with changes in their circadian rhythmicity. In
380 addition, pseudogenization of these genes possibly paralleled loss of other circadian
381 rhythm related genes, namely Cortistatin gene, that encodes a pleiotropic
382 neuropeptide with an important role in sleep physiology (Valente et al., 2021). Given
383 that the evolution of melatonin-related genes should be directly linked with pineal
384 gland function, by inferring their coding status we were able to deduce if the organ
385 constitutes an evolutionary vestige, despite the conflicting anatomical reports. More
386 importantly, the present study provides a clear case-study on how genomic data can

387 be used to disentangle whether a specific organ constitutes a functional or vestigial
388 structure (Hiller et al., 2012).

389

390 **5. Conclusion**

391 To date, no unequivocal inferences on the functional status of pineal gland across
392 mammals were provided, with anatomical observations in several species from
393 different clades presenting conflicting conclusions. However, by making use of
394 genomic data, our results provide solid evidence for pineal gland vestigiality not only
395 in Xenarthra, but also in other mammalian lineages. Thus, we argue that analysis of
396 genomic changes might constitute a powerful approach to gain insights into the
397 vestigiality of specific organs.

398

399 **. Funding**

400 This work is a result of the project ATLANTIDA (ref. NORTE-01-0145-FEDER-000040),
401 supported by the Norte Portugal Regional Operational Programme (NORTE 2020),
402 under the PORTUGAL 2020 Partnership Agreement and through the European
403 Regional Development Fund (ERDF). One PhD fellowship for author R.V.
404 (SFRH/BD/144786/2019) was granted by Fundação para a Ciência e Tecnologia (FCT,
405 Portugal) under the auspices of Programa Operacional Regional Norte (PORN),
406 supported by the European Social Fund (ESF) and Portuguese funds (MECTES).

407

408 **. Author's contributions**

409 **Raul Valente:** Data curation, Formal analysis, Investigation, Methodology,
410 Visualization, Writing - original draft **Filipe Alves:** Writing - review & editing **Isabel**
411 **Sousa-Pinto:** Writing - review & editing **Raquel Ruivo:** Conceptualization,
412 Methodology, Validation, Writing - review & editing **Luís Filipe Costa de Castro:**
413 Conceptualization, Methodology, Validation, Supervision, Project administration,
414 Resources, Writing - review & editing

415

416 **. Acknowledgements**

417 We acknowledge the various genome consortiums for sequencing and assembling
418 the genomes.

419

420 **. Declaration of Competing Interest**

421 The authors declare that they have no competing interests.

422

423 **. References**

424

425 Albalat, R., Cañestro, C., 2016. Evolution by gene loss. *Nat. Rev. Genet.* 17, 379–391.

426 <https://doi.org/10.1038/nrg.2016.39>

427

428 Allmon, W.D., Ross, R.M., 2018. Evolutionary remnants as widely accessible evidence
429 for evolution: the structure of the argument for application to evolution education.

430 *Evol. Educ. Outreach* 11, 1. <https://doi.org/10.1186/s12052-017-0075-1>

431

432 Alves, L.Q., Alves, J., Ribeiro, R., Ruivo, R., Castro, F. 2019. The dopamine receptor D5
433 gene shows signs of independent erosion in toothed and baleen whales. *PeerJ* 7,
434 e7758. <https://doi.org/10.7717/peerj.7758>

435

436 Alves, L.Q., Ruivo, R., Fonseca, M.M., Lopes-Marques, M., Ribeiro, P., Castro, L.F.C.,
437 2020. PseudoChecker: an integrated online platform for gene inactivation inference.
438 *Nucleic Acids Res.* 48, W321–W331. <https://doi.org/10.1093/nar/gkaa408>

439

440 Attias, N., Oliveira-Santos, L.G.R, Fagan, W.F., Mourão, G., 2018. Effects of air
441 temperature on habitat selection and activity patterns of two tropical imperfect
442 homeotherms. *Animal Behav.* 140, 129–140.

443

444 Axelrod, J., Wurtman, R.J., Winget, C.M., 1964. Melatonin synthesis in the Hen pineal
445 and its control by light. *Nature* 201, 1134.

446

447 Benítez, I., Aldana Marcos, H.J., Affanni, J.M., 1994. The encephalon of
448 *Chaetophractus villosus*. A general view of its most salient features. *Comun. Biol.* 12,
449 57–73.

450

- 451 Castro, L.F.C., Gonçalves, O., Mazan, S., Tay, B.-H., Venkatesh, B., Wilson, J.M., 2014.
452 Recurrent gene loss correlates with the evolution of stomach phenotypes in gna-
453 thostome history. *Proc. R. Soc. B: Biol. Sci.*, 281
454
- 455 Camilo-Alves, C.S.P., Mourão, G.M., 2006. Responses of a specialized insectivorous
456 mammal (*Myrmecophaga tridactyla*) to variation in ambient temperature. *Biotropica*
457 38, 52–56.
458
- 459 Chiarello, A.G., 1998. Activity budgets and ranging patterns of the Atlantic forest
460 maned sloth *Bradypus torquatus* (Xenarthra: Bradypodidae). *J. Zool.* 246, 1–10.
461
- 462 Cronk, Q., 2009. *The Molecular Organography of Plants*. Oxford University Press,
463 Oxford.
464
- 465 Darwin, C., 1859. *On the origin of species by means of natural selection or the*
466 *preservation of favoured races in the struggle of life*. John Murray Press, London.
467
- 468 Di Blanco, Y.E., Spørring, K.L., Di Bitetti, M.S., 2017. Daily activity pattern of re-
469 introduced giant anteaters (*Myrmecophaga tridactyla*): effects of seasonality and
470 experience. *Mammalia* 81, 11–21.
471
- 472 Eisenberg, J.F., Redford, K.H., 1999. *Mammals of the Neotropics*. vol. 3, the central
473 Neotropics: Ecuador, Peru, Bolivia, Brazil. University of Chicago Press, Chicago.
474
- 475 Esfeld, K., Berardi, A.E., Moser, M., Bossolini, E., Freitas, L., Kuhlemeier, C., 2018.
476 Pseudogenization and resurrection of a speciation gene. *Curr. Biol.* 28, 3776–3786.
477
- 478 Fang, X., Seim, I., Huang, Z., Gerashchenko, M.V., Xiong, Z., Turanov, A.A., Zhu, Y.,
479 Lobanov, A.V., Fan, D., Yim, S.H., Yao, X., Ma, S., Yang, L., Lee, S., Buffenstein, R.,
480 Zhou, X., Krogh, A., Kim, E.B., Bronson, R.T., Sumbera, R., Park, T.J., Zhang, G., Wang,
481 J., Gladyshev, V.N., 2014. Adaptations to a subterranean environment and longevity
482 revealed by the analysis of mole rat genomes. *Cell Rep.* 8, 1–11.

483

484 Ferrari, C.C., Marcos, H.J.A., Carmanchahi, P.D., Benítez, I., Affanni, J.M., 1998. The
485 Brain of the Armadillo *Dasypus hybridus*. A general view of its most salient features.
486 Biocell, 22, 123–140.

487

488 Freitas, L.M., dos Santos, O.P., Santos, A.L.Q., Rodrigues de Melo, F., Silveira, L.,
489 Jácomo, A.T.A., Pereira, K.F., Lima, F.C., 2019. Brain anatomy of two-toed sloth
490 (*Choloepus didactylus*, Linnaeus, 1758): A comparative gross anatomical study of
491 extant xenarthrans. Anat. Histol.
492 Embryol. 49, 130–143. <https://doi.org/10.1111/ahe.12501>

493

494 Giné, G.A.F., Cassano, C.R., de Almeida, S.S., Faria, D., 2015. Activity budget, pattern
495 and rhythm of maned sloths (*Bradypus torquatus*): responses to variations in ambient
496 temperature. Mammal Biol. 80, 459–467.
497 <https://doi.org/10.1016/j.mambio.2015.07.003>

498

499 Greegor, D.H.Jr., 1985. Ecology of the little hairy armadillo *Chaetophractus vellerosus*.
500 In: Montgomery, G.G. (Eds.), The evolution and ecology of armadillos, sloths and
501 vermilinguas. Smithsonian Institution Press, Washington D.C., pp. 397–405.

502

503 Guijarro-Clarke, C., Holland, P.W.H., Paps, J. 2020. Widespread patterns of gene loss
504 in the evolution of the animal kingdom. Nat. Ecol. Evol. 4, 519–523.
505 <https://doi.org/10.1038/s41559-020-1159-9>

506

507 Harlow, H.J., Phillips, J.A., Ralph, C.L., 1981. Daynight rhythm in plasma melatonin in a
508 mammal lacking a distinct pineal gland, the nine-banded armadillo. Gen. Comp.
509 Endocrinol. 45, 212–218. [https://doi.org/10.1016/0016-6480\(81\)90106-4](https://doi.org/10.1016/0016-6480(81)90106-4)

510

511 Harlow, H.J., Phillips, J.A., Ralph, C.L., 1982. Circadian rhythms and the effects of
512 exogenous melatonin in the ninebanded armadillo, *Dasypus novemcinctus*: a mammal
513 lacking a distinct pineal gland. Physiol. Behav. 29, 307–313.

514

- 515 Heath, M.E., Hammel, H.T., 1986. Body temperature and rate of O₂ consumption in
516 Chinese pangolins. *Am. J. Physiol. Regul. Integr. Comp. Physiol.* 250, 377–382.
517
- 518 Hiller, M., Schaar, B.T., Indjeian, V.B., Kingsley, D.M., Hagey, L.R., Bejerano G, 2012. A
519 “forward genomics” approach links genotype to phenotype using independent
520 phenotypic losses among related species. *Cell Rep.* 2(4), 817–23.
521
- 522 Huelsmann, M., Hecker, N., Springer, M.S., Gatesy, J., Sharma, V., Hiller, M., 2019.
523 Genes lost during the transition from land to water in cetaceans highlight genomic
524 changes involved in aquatic adaptations. *Sci. Adv.* 5 (9), eaaw6671.
525 <https://doi.org/10.1126/sciadv.aaw6671>
526
- 527 Imam, A., Bhagwandin, A., Ajao, M.S., Manger, P.R., 2018. The brain of the tree
528 pangolin (*Manis tricuspis*). V. The diencephalon and hypothalamus. *J. Comp. Neurol.*
529 527, 2413–2439. <https://doi.org/10.1002/cne.24619>
530
- 531 Jacob, S., Zelano, B., Gungor, A., Abbott, D., Naclerio, R., McClintock, M.K., 2000.
532 Location and gross morphology of the nasopalatine duct in human adults. *Arch.*
533 *Otolaryngol. Head Neck Surg.* 126, 741–748.
534
- 535 Kim, E.B., Fang, X., Fushan, A.A., Huang, Z., Lobanov, A.V., Han, L., Marino, S.M., Sun,
536 X., Turanov, A.A., Yang, P., Yim, S.H., Zhao, X., Kasaikina, M.V., Stoletzki, N., Peng, C.,
537 Polak, P., Xiong, Z., Kiezun, A., Zhu, Y., Chen, Y., Kryukov, G.V., Zhang, Q., Peshkin, L.,
538 Yang, L., Bronson, R.T., Buffenstein, R., Wang, B., Han, C., Li, Q., Chen, L., Zhao, W.,
539 Sunyaev, S.R., Park, T.J., Zhang, G., Wang, J., Gladyshev, V.N., 2011. Genome
540 sequencing reveals insights into physiology and longevity of the naked mole rat.
541 *Nature* 479, 223–227.
542
- 543 Klein, D., Coon, S., Roseboom, P., Weller, J.L., Bernard, M., Gastel, J.A., Zatz, M.,
544 Iuvone, P., Rodriguez, I., Bégay, V., Falcón, J., Cahill, G.M., Cassone, V.M., Baler, R.,
545 1997. The melatonin rhythm-generating enzyme: Molecular regulation of serotonin
546 N-acetyltransferase in the pineal gland. *Recent Prog. Horm. Res.* 52, 307–357.

547

548 Lewy, A.J., Wehr, T.A., Goodwin, F.K., Newsome, D.A., Markey, S.P., 1980. Light
549 suppresses melatonin secretion in humans. *Science* 210, 1267 – 1269.

550

551 Lindblad-Toh, K., Garber, M., Zuk, O., Lin, M.F., Parker, B.J., Washietl, S., Kheradpour,
552 P., Ernst, J., Jordan, G., Mauceli, E., et al., 2011. A high-resolution map of human
553 evolutionary constraint using 29 mammals. *Nature* 478, 476–482.

554

555 Lopes-Marques, M., Machado, A.M., Alves, L.Q., Fonseca, M.M., Barbosa, S., Sinding
556 M-H.S., Rasmussen, M.H., Iversen, M.R., Bertelsen, M.F., Campos, P.F., Da Fonseca,
557 R., Ruivo, R., Castro, L.F.C., 2019a. Complete inactivation of sebum-producing genes
558 parallels the loss of sebaceous glands in Cetacea. *Mol. Biol. Evol.* 36 (6), 1270–1280.
559 <https://doi.org/10.1093/molbev/msz068>.

560

561 Lopes-Marques, M., Ruivo, R., Alves, L.Q., Sousa, N., Machado, A.M., Castro, L.F.C.,
562 2019b. The singularity of Cetacea behavior parallels the complete inactivation of
563 melatonin gene modules. *Genes* 10(2), 121. <https://doi.org/10.3390/genes10020121>

564

565 Lopes-Marques, M., Alves, L.Q., Fonseca, M.M., Secci-Petretto, G., Machado, A.M.,
566 Ruivo, R., Castro, L.F.C. 2019c. Convergent inactivation of the skin-specific CC motif
567 chemokine ligand 27 in mammalian evolution. *Immunogenetics* 71(5), 363–372.
568 <https://doi.org/10.1007/s00251-019-01114-z>

569

570 Maccarini, T.B., Attias, N., Medri, I.M., Marinho-Filho, J., Mourão, G.M., 2015.
571 Temperature influences the activity patterns of armadillo species in a large
572 neotropical wetland. *Mamm. Res.* 60, 403–409.

573

574 McGaugh, S.E., Gross, J.B., Aken, B., Blin, M., Borowsky, R., Chalopin, D., Hinaux, H.,
575 Jeffery, W.R., Keene, A., Ma, L., Minx, P., Murphy, D., O’Quin, K.E., Rétaux, S., Rohner,
576 N., Searle, S.M.J., Stahl, B.A., Tabin, C., Volff, J.-N., Yoshizawa, M., Warren, W.C., 2014.
577 The cavefish genome reveals candidate genes for eye loss. *Nat Commun.* 5, 5307.

578

- 579 Mc Nab, B.K., 1979. The influence of body size on the energetics and distribution of
580 fossorial and burrowing mammals. *Ecology* 60, 1010–1021.
581
- 582 Mc Nab, B.K., 1980. Energetics and the limits to a temperate distribution in armadillos.
583 *J. Mammal.* 61, 606–627.
584
- 585 Mc Nab, B.K., 1984. Physiological convergence amongst ant-eating and termite-
586 eating mammals. *J. Zool. (Lond.)* 203, 485–510.
587
- 588 Mc Nab, B.K., 1985. Energetics, population biology and distribution of xenarthrans
589 living and extinct. In: Montgomery, G.G. (Ed.), *The Evolution and Ecology of*
590 *Armadillos, Sloths and Vermilinguas*. Smithsonian Institution Press,
591 Washington/London, pp. 219–232.
592
- 593 Murphy, W.J., Pringle, T.H., Crider, T.A., Springer, M.S., Miller, W., 2007. Using
594 genomic data to unravel the root of the placental mammal phylogeny. *Genome Res.*
595 17, 413–421.
596
- 597 Nweeia, M.T., Eichmiller, F.C., Hauschka, P.V., Tyler, E., Mead, J.G., Potter, C.W.,
598 Angnatsiak, D.P, Richard, P.R., Orr, J.R., Black, S.R., 2012. Vestigial tooth anatomy and
599 tusk nomenclature for *Monodon monoceros*. *Anat. Rec.* 295, 1006–1016.
600
- 601 Oksche, A., 1965. Survey of the development and comparative morphology of the
602 pineal organ. *Prog. Brain Res.* 10, 3–29.
603
- 604 O’Leary, M.A., Bloch, J.I., Flynn, J.J., Gaudin, T.J., Giallombardo, A., Giannini, N.P.,
605 Goldberg, S.L., Kraatz, B.P., Luo, Z.-X., Meng, J., et al., 2013. The placental mammal
606 ancestor and the post-K-Pg radiation of placentals. *Science* 339, 662–667.
607
- 608 Olson, M.V., 1999. When less is more: gene loss as an engine of evolutionary change.
609 *Am. J. Hum. Genet.* 64, 18–23.
610

- 611 Panin, M., Gabai, G., Ballarin, C., Peruffo, A., Cozzi, B, 2012. Evidence of melatonin
612 secretion in cetaceans: Plasma concentration and extrapineal HIOMT-like presence in
613 the bottlenose dolphin *Tursiops truncatus*. *Gen. Comp. Endocrinol.* 177, 238–245.
614
- 615 Pévet, P., 2002. Melatonin. *Dialogues Clin. Neurosci.* 4, 57–72.
616
- 617 Quay, W., 1965. Histological structure and cytology of the pineal organ in birds and
618 mammals. In: Kappers, J., Schade, J. (Eds.), *Progress in brain research, Structure and*
619 *function of the epiphysis Cerebri*, vol 10. Elsevier, New York, pp. 49–
620 86. [https://doi.org/10.1016/S0079-6123\(08\)63447-0](https://doi.org/10.1016/S0079-6123(08)63447-0)
621
- 622 Ralph, C.L., 1975. The pineal gland and geographical distribution of animals. *Int. J.*
623 *Biometeorol.* 19, 289–303.
624
- 625 Ralph, C.L., Young, S., Gettinger, R., O’Shea, T.J., 1985. Does the manatee have a
626 pineal body? *Acta Zool.* 66, 55–60.
627
- 628 Reppart, S.M., Weaver, D.R., Godson, C., 1996. Melatonin receptors step into the
629 light: Cloning and classification of subtypes. *Trends Pharmacol. Sci.* 17, 100–102.
630
- 631 Simonneaux, V., Ribelayga, C., 2003. Generation of the melatonin endocrine message
632 in mammals: A review of the complex regulation of melatonin synthesis by
633 norepinephrine, peptides, and other pineal transmitters. *Pharmacol. Rev.* 55, 325.
634
- 635 Slominski, A., Pisarchik, A., Semak, I., Sweatman, T., Wortsman, J., 2003.
636 Characterization of the serotonergic system in the C57BL/6 mouse skin. *Eur. J.*
637 *Biochem.* 270, 3335–3344.
638
- 639 Springer, M.S., Guerrero-Juarez, C.F., Huelsmann, M., Collin, M.A., Danil, K.,
640 McGowen, M.R., Oh, J.W., Ramos, R., Hiller, M., Plikus, M.V., Gatesy, J., 2021. Genomic
641 and anatomical comparisons of skin support independent adaptation to life in water
642 by cetaceans and hippos. *Current Biology* (in press).

643

644 Superina, M., Loughry, W.J., 2015. Why do xenarthrans matter? *J. Mammal.* 96, 617–
645 621. <https://doi.org/10.1093/jmammal/gyv099>

646

647 Tan, D.X., Hardeland, R., Manchester, L.C., Paredes, S.D., Korkmaz, A., Sainz, R.M.,
648 Mayo, J.C., Fuentes-Broto, L., Reiter, R.J., 2010. The changing biological roles of
649 melatonin during evolution: From an antioxidant to signals of darkness, sexual
650 selection and fitness. *Biol. Rev. Camb. Philos. Soc.* 85, 607–623.

651

652 Tan, D.X., Hardeland, R., Back, K., Manchester, L.C., Alatorre-Jimenez, M.A., Reiter,
653 R.J., 2016. On the significance of an alternate pathway of melatonin synthesis via 5-
654 methoxytryptamine: Comparisons across species. *J. Pineal Res.* 61, 27–40.

655

656 Themudo, G.E., Alves, L.Q., Machado, A.M., Lopes-Marques, M., da Fonseca, R.R.,
657 Fonseca, M., et al. (2020). Losing genes: the evolutionary remodeling of Cetacea skin.
658 *Front. Mar. Sci.* 7, 912.

659

660 Uliano-Silva, M., Winkler, S., Myers, E., Mazzoni, C., 2019. Slothomics: the first
661 chromosome-level genome of the slowest existing mammalian group. The G10K-
662 VGP/EBP 2019 Meeting Agenda, Manhattan, New York, August 2019. Poster
663 presentation

664

665 Valente, R., Alves, L.Q., Nabais, M., Alves, F., Sousa-Pinto, I., Ruivo, R., Castro, L.F.C.,
666 (2021). Convergent Cortistatin losses parallel modifications in circadian rhythmicity
667 and energy homeostasis in Cetacea and other mammalian lineages. *Genomics* 113(1),
668 1064-1070. <https://doi.org/10.1016/j.ygeno.2020.11.002>

669

670 Vazquez, J.M., Sulak, M., Chigurupati, S., Lynch, V.J., 2018. A zombie LIF gene in
671 elephants is upregulated by TP53 to induce apoptosis in response to DNA damage.
672 *Cell Rep.* 24 (7), 1765–1776.

673

674 Weber, R.E., Heath, M.E., White, F.N., 1986. Oxygen binding functions of blood and
675 hemoglobin from the Chinese pangolin, *Manis pentadactyla*: possible implications of
676 burrowing and low body temperature. *Respir. Physiol.* 64, 103–112.

677

678 Werth, A.J., 2014. Vestiges of the natural history of development: historical holdovers
679 reveal the dynamic interaction between ontogeny and phylogeny. *Evol. Educ.*
680 *Outreach* 7, 12. <https://doi.org/10.1186/s12052-014-0012-5>

681

682 Yin, D., Zhou, R., Yin, M., Chen, Y., Xu, S., Yang, G., 2021. Gene duplication and loss of
683 AANAT in mammals driven by rhythmic adaptations, *Mol. Biol. Evol.* msab125.
684 <https://doi.org/10.1093/molbev/msab125>

685

686 Zoonomia Consortium, 2020. A comparative genomics multitool for scientific
687 discovery and conservation. *Nature* 587, 240–245. [https://doi.org/10.1038/s41586-](https://doi.org/10.1038/s41586-020-2876-6)
688 [020-2876-6](https://doi.org/10.1038/s41586-020-2876-6)